arXiv:1607.03772v2 [cond-mat.stat-mech] 27 Sep 2016

Critical drying of liquids

Robert Evans,[1] Maria C. Stewart,[1] and Nigel B. Wilding[2]

[1] *H. H. Wills Physics Laboratory, University of Bristol, Royal Fort, Bristol BS8 1TL, United Kingdom.*
[2] *Department of Physics, University of Bath, Bath BA2 7AY, United Kingdom.*

We report a detailed simulation and classical density functional theory study of the drying transition in a realistic model fluid at a smooth substrate. This transition (in which the contact angle $\theta \to 180^\circ$) is shown to be critical for both short ranged and long-ranged substrate-fluid interaction potentials. In the latter case critical drying occurs at exactly zero attractive substrate strength. This observation permits the accurate elucidation of the character of the transition via a finite-size scaling analysis of the density probability function. We find that the critical exponent $\nu_\parallel$ that controls the parallel correlation length, i.e. the extent of vapor bubbles at the wall, is over twice as large as predicted by mean field and renormalization group calculations. We suggest a reason for the discrepancy. Our findings shed new light on fluctuation phenomena in fluids near hydrophobic and solvophobic interfaces.

With new types of nanostructured hydrophobic substrates and coatings finding application in systems such as microfluidic devices, self-cleaning surfaces and chemical separation processes, there is considerable interdisciplinary interest in the behavior of fluids in contact with weakly attractive surfaces [1–4]. Thermodynamically, the state of a liquid drop near a solid substrate (or 'wall') is characterized by the contact angle θ that the drop makes with the surface. The weaker the wall-fluid attraction, the larger θ becomes. In the limit $\theta \to 180^\circ$ a fluid at vapor-liquid coexistence undergoes a surface phase transition known as *drying* whereby a macroscopic film of vapor (v) intrudes between the wall (w) and the bulk liquid (l); this is the analogue of the well known wetting transition that occurs for strongly attractive surfaces as $\theta \to 0$. Wetting has been studied in detail; see [5] for a review and [6] for a recent investigation of water. Theory and simulation has often focused on Ising models e.g. [7–9], whose special symmetry implies that wetting and drying are equivalent. However in real fluids, wetting and drying are distinct phenomena and very little is known concerning the fundamental properties of either transition. Previous work has led to long standing controversies in particular as to whether the drying transition in model fluids is first order or continuous (critical) [10–16], or even whether it exists at all [17, 18]. Accordingly there is a need for clear elucidation of the nature of the approach to drying in fluids, not just in thermodynamic terms, but also with regard to the local density fluctuations that characterize the transition.

The main barriers to computational progress in tackling drying in realistic fluids has been the dearth of techniques for locating surface phase transitions accurately, combined with the lack of rigorous measures for quantifying their key characteristics. In this Letter we deploy state-of-the-art Monte Carlo simulation techniques and classical density functional theory (DFT) together with a rigorously defined measure of the local compressibility to study a realistic model fluid near an attractive structureless wall. We begin by settling the long standing controversy concerning the order of the drying transition: For the (truncated) Lennard-Jones (LJ) fluid that we consider, drying is continuous (critical). This is true for both a short-ranged (SR) and a long-ranged (LR) van der Waals wall-fluid interaction potential –a finding that contrasts with wetting in the same system which is a discontinuous transition for the LR wall-fluid potential but continuous for the SR case. Moreover, we show that for LR wall-fluid potentials, drying occurs at *zero* attractive wall strength. This represents the first instance of a surface phase transition in 3d whose parameters are exactly known and thus provides an opportunity to study a surface critical point free from uncertainty regarding its location (a problem that has previously plagued Ising model studies of critical wetting [9]). By performing a finite size scaling (FSS) analysis of the density fluctuations that characterize the near critical region in the LR case, we demonstrate that critical drying in simulations is associated with a *single* divergent correlation length $\xi_\parallel$, that for density correlations parallel to the wall. The interfacial roughness $\xi_\perp$, arising from capillary wave fluctuations, is heavily dampened by finite-size effects to of order the particle diameter and plays no role in the FSS. Our analysis allows us to estimate the effective critical exponent $\nu_\parallel$ describing the growth of $\xi_\parallel$. We note that our 3d system is at the upper critical dimension and, in contrast to the case of SR wall-fluid interactions, a renormalization group (RG) analysis indicates [19] that the critical exponents should take their mean-field values. However, our simulation estimate of $\nu_\parallel$ is much larger than that predicted by mean-field and furthermore appears to be temperature dependent.

The model we consider is a LJ fluid in a slit pore composed of a pair of structureless parallel walls of area L^2 separated by a distance D; periodic boundary conditions apply in the directions parallel to the walls. Fluid-fluid interactions are truncated at $r_c = 2.5\sigma$, where σ is the LJ diameter, and particles interact with each wall via a wall-fluid potential $W(z)$, with z the perpendicular particle-wall distance. We consider two forms for $W(z)$ commonly

encountered in the adsorption literature: (i) the SR case of a hard wall plus square well potential of range 0.5σ, and, (ii) the LR case of a hard wall plus a non-truncated long-ranged attraction decaying as z^{-3}. Both wall-fluid potentials are parameterized in terms of the well depth ϵ. To study these systems we deploy Grand Canonical Monte Carlo (GCMC) simulation and classical DFT. The latter approximates the repulsive LJ core as a hard core, whose free energy is treated via fundamental measure theory, while the attractive part of the LJ potential is treated in a mean field fashion [19–21]. The GCMC simulations impose the temperature T, chemical potential μ and the depth ϵ of $W(z)$, which we quote in units of k_BT. Flat histogram techniques [22] were used to record the local number density profile $\rho(z)$ and the overall number density ρ. All results were accumulated at liquid-vapor coexistence for two subcritical temperatures $T = 0.775T_c$ and $T = 0.842T_c$, with T_c the bulk critical temperature known from previous work [23]. The coexistence value of μ was determined to high precision for a large fully periodic system using recently developed bespoke techniques [24] which ameliorate the sampling problems at low T and large volumes that arise from 'droplet' transitions [25].

The dependence of the contact angle on the wall-fluid well depth ϵ was estimated for both the SR and LR wall-fluid potentials via direct measurements of the interfacial tensions appearing in Young's equation, $\gamma_{lv}\cos(\theta) = \gamma_{wv} - \gamma_{wl}$, using a method detailed elsewhere [26, 27]. The results are shown in Fig. 1 and span the range from wetting ($\cos(\theta) = 1$) to drying ($\cos(\theta) = -1$). Interestingly the two forms of wall-fluid potential show distinct behavior. For the SR case, both wetting and drying are continuous for this range of $W(z)$: $\cos(\theta)$ approaches the respective limits tangentially [28]. For the LR case, the same is true for drying, but wetting is first order: $\cos(\theta)$ approaches unity with a non-zero linear slope. The DFT results in Fig. 1 display the same transitions as in simulation.

In what follows we focus on drying in the LR case which is the situation most commonly studied in simulations of LJ fluids [29–31] and of models of water [32–34]. From Fig. 1 it appears at first sight that here drying occurs at a non-zero (albeit small) value of ϵ. However, while measurements of $\cos(\theta)$ are reliable indicators of the order of the transitions, they fail to provide accurate estimates for the critical well depth ϵ_c. The problem goes well beyond that of the inherent difficulty of determining the point at which $\cos(\theta) = -1$ when the approach to this limit is tangential. Instead the main issue is one of critical finite-size effects which systematically shift the apparent critical point with respect to its true value. Accordingly a FSS analysis of the near-critical fluctuations is vital for determining accurately the drying point.

Our approach is to examine the probability distribution function of the number density $p(\rho)$, and specifically

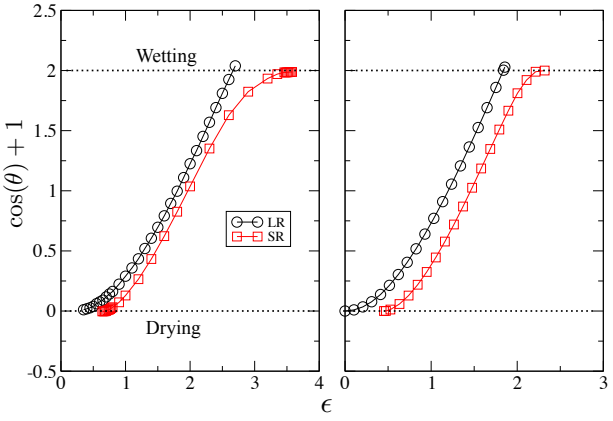

FIG. 1. (Color online) Left: GCMC results for $\cos(\theta) + 1$ versus ϵ for the SR and LR wall potential at $T = 0.775T_c$, for $L = 15\sigma, D = 30\sigma$. For the LR case a FSS analysis of the GCMC data yields critical drying at $\epsilon_c = 0$, as predicted by theory while for the SR case a FSS analysis gives critical drying at $\epsilon_c = 0.52(2)$ and critical wetting at $\epsilon_c = 4.25(5)$. Right: Corresponding DFT results.

its dependence on ϵ and the wall dimension L. Results are shown in Fig. 2 and reveal that for sufficiently large ϵ and L, $p(\rho)$ exhibits a peak at high density. In the absence of finite-size effects, this peak corresponds to the liquid phase in contact with the wall and is a signature of partial drying ie. $\theta < 180°$. However, the situation is more subtle. On decreasing ϵ, the peak in $p(\rho)$ disappears into a plateau. On further reducing ϵ, $p(\rho)$ becomes monotonically decreasing with a bulge which gradually diminishes until, at $\epsilon = 0$, the distribution comprises a linear part and a tail. The range of values of ϵ over which this scenario plays out decreases with increasing L. Only for $\epsilon = 0$ is the form of $p(\rho)$ scale invariant, ie. no peak begins to form as L is increased. Consequently this wall strength marks the critical drying point. Significantly, both DFT (c.f. fig. 1) and binding potential calculations [19] also predict critical drying for $\epsilon = 0$. When $\epsilon = 0$, $W(z)$ reduces to the hard wall potential and complete drying occurs for all $T < T_c$. What is remarkable is that the transition is critical and occurs precisely at $\epsilon = 0$ for all $W(z)$ exhibiting power-law decay [19].

The fact that for a LR wall potential drying is critical with $\epsilon_c = 0$ is confirmed by measurements of the compressibility profile $\chi(z) \equiv \partial\rho(z)/\partial\mu$. This quantity was introduced previously [35, 36] and has subsequently proven a sensitive measure of the link between the contact angle θ and the local structure near hydrophobic or solvophobic surfaces [21, 27]. Its form probes the transverse density-density correlation function and thus the correlation length $\xi_\parallel$. GCMC measurements of the maximum of $\chi(z)$ are shown in Fig. 3 and demonstrate a power law divergence as ϵ is reduced to zero, implying that $\xi_\parallel$ diverges at this wall strength. This divergence is confirmed by DFT measurements of $\chi(z)$ as shown in

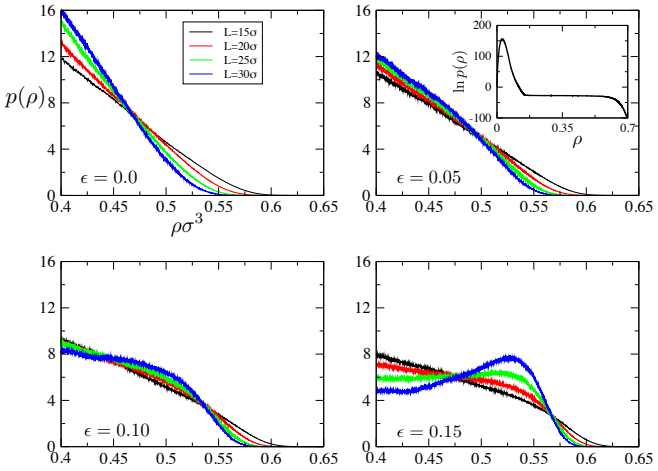

FIG. 2. (Color online) GCMC results for $p(\rho)$ for the LR wall potential for $D = 30\sigma$ and various L at a selection of near-critical values of ϵ. Note that at small ρ capillary evaporation occurs, manifest as a gas-like peak in $p(\rho)$ as shown in the inset for $\epsilon = 0.05, L = 15\sigma$.

the inset.

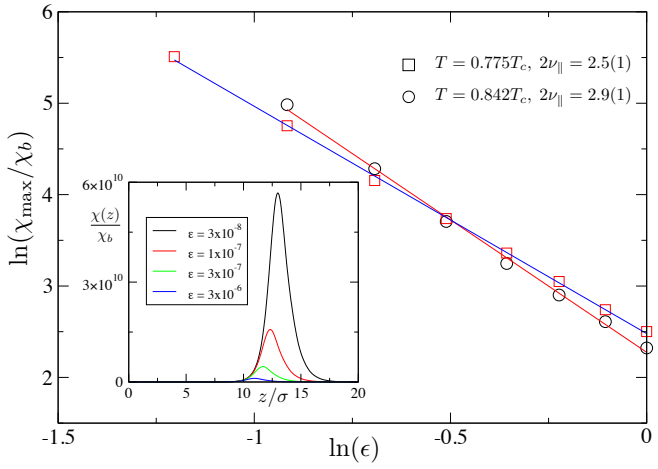

FIG. 3. (Color online) GCMC measurements of the scaling of the peak in $\chi(z)/\chi_b$ with wall-fluid potential well depth ϵ for the LR wall-fluid potential. χ_b is the bulk liquid phase compressibility. The system size is $L = 50\sigma, D = 30\sigma$. Inset: DFT results for $\chi(z)/\chi_b$ for a single wall, showing the divergence as $\epsilon \to 0$. This occurs in the way binding potential arguments predict, i.e. $\ln(\chi(l)) \sim l$ with l the drying layer thickness and $\chi(l) \sim \xi_\parallel^2$, see fig. S1. of [19].

The form of $p(\rho)$ at $\epsilon = 0$ (Fig. 2), corresponding to a hard wall, represents a hallmark of critical drying and yields fundamental insight concerning its character. It comprises a linearly sloped part at lower density plus a tail at higher densities. With increasing L, the tail density shifts to lower values. Interestingly, the form and L-dependence of $p(\rho|\epsilon_c)$ cannot be rationalized in terms of a FSS ansatz previously proposed for critical wetting in $3d$ Ising models [8, 9]. That theory presumes the critical divergence of not just $\xi_\parallel$, but also of the perpendicular correlation length $\xi_\perp$ which measures the roughness of the emerging liquid-vapor interface due to capillary fluctuations. While our measurements of $\chi(z)$ provide ample evidence for a divergent $\xi_\parallel$, we find no signs that $\xi_\perp$ is large in our simulations. This is because of the extremely strong finite-size dampening of the surface roughness for $d = 3$. General capillary wave arguments e.g. [20, 28, 37] for a single unbinding vapor-liquid interface predict that $\xi_\perp \simeq \sqrt{(k_BT/2\pi\gamma_{lv})\ln(L/\xi_b)}$. Thus the interfacial roughness depends on the finite *lateral* dimension of the system. Given the strength of this dampening, one cannot expect $\xi_\perp$ to become large on the scale of the particle diameter (or indeed the bulk correlation length ξ_b) for currently accessible simulation sizes.

These observations, together with the results of Figs. 2 and 3, imply the following picture for critical drying in simulations of 3d systems. As $\epsilon \to \epsilon_c^+$, bubbles of vapor form at the wall whose lateral size corresponds to $\xi_\parallel \sim (\epsilon - \epsilon_c)^{-\nu_\parallel}$ (cf. the snapshot in fig. 4 and the movie in the SM[19]), but whose perpendicular length-scale remains microscopic. As $\xi_\parallel$ approaches L, the liquid unbinds from the wall to form a 'slab', surrounded by vapor. Essentially this process can be viewed as premature drying induced by the finite system size. The slab surface is rather sharp and localized due to the dampening of interfacial roughness and the slab thickness (in the z-direction) is therefore proportional to ρ. Accordingly, the linear decrease of $p(\rho|\epsilon = 0)$ seen at low to moderate densities in fig. 2 arises simply from the 'entropic repulsion' of the slab and the wall: the number of positions for the slab center along the z axis that are allowed by the presence of the wall, varies linearly with slab thickness. The high density tail of $p(\rho)$ on the other hand reflects the free energy cost of pushing the liquid up against the wall, the act of which quenches the parallel density fluctuations. Its L dependence arises –as shown in the SM [19]– from a constant repulsive pressure on the liquid-vapor interface by the wall, giving rise to a force which scales simply with the wall area L^2.

Neither the fluctuation in the thickness of the unbound liquid slab occurring at low-moderate densities, nor the high density tail is directly associated with criticality, and thus one cannot expect $p(\rho)$ to exhibit non-trivial FSS behavior as a whole. Rather, the signature of near critical fluctuations is manifest in the density range where the liquid is still (weakly) bound to the wall but exhibits strong parallel density fluctuations. This correspond to the liquid peak in Fig. 2, the height of which depends on $\xi_\parallel$ and vanishes when $\xi_\parallel \approx L$ allowing the liquid slab to unbind from the wall. Simple FSS dictates that this vanishing occurs not at ϵ_c but at the larger effective value $\epsilon_c(L) = \epsilon_c + aL^{-1/\nu_\parallel}$ (which corresponds also to the wall strength at which the surface tension measurements with Young's equation, predict $\theta = 180°$). The critical wall

strength ϵ_c can differ substantially from $\epsilon_c(L)$ and is determined most accurately as the largest value of ϵ for which $p(\rho)$ assumes an L-independent form. However, in contrast to the rich structure of the density distribution at bulk criticality [23] the novel feature of critical drying is the surprising simplicity of $p(\rho|\epsilon_c)$.

We have determined the value of $\nu_\parallel$ via the anticipated FSS $\epsilon(L) \sim L^{-1/\nu_\parallel}$; $\epsilon_c = 0$ for the LR case. For a number of choices of L we measured $\epsilon(L)$ accurately (using histogram extrapolation techniques) from the vanishing of the liquid peak of $p(\rho)$ (cf. fig. 2). As fig. 4 shows, we do indeed see power law scaling, from which we can extract an estimate of $\nu_\parallel$. Interestingly, however, this estimate exceeds the prediction $\nu_\parallel = 0.5$ of mean field and RG theories (see SM [19]) by over a factor of two and additionally appears to show a clear temperature dependence. This discrepancy with theory is further mirrored in the behavior of $\chi(z)$ (fig. 3) for which one expects [19] that $\chi_{\max} \sim (\epsilon - \epsilon_c)^{-2\nu_\parallel}$. Here too the simulation estimates of $\nu_\parallel$ are over twice the theoretical prediction and show a clear temperature dependence.

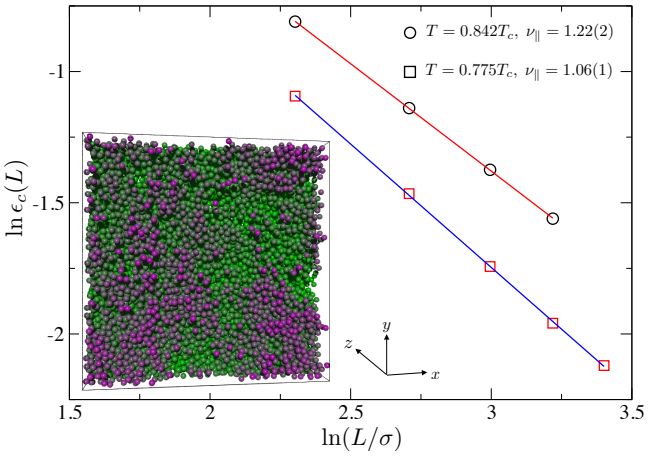

FIG. 4. The scaling of $\epsilon_c(L)$, i.e. the wall strength at which a peak appears in $p(\rho)$, as a function of L for the LR wall-fluid potential. Data are shown for two subcritical temperatures. Inset: Simulation snapshot for a system with $L = 40\sigma, \epsilon = 0.2$. Particles are color coded according to their distance from the wall at $z = 0$. A large correlation length is manifest in the vapor close to the wall; see SM [19].

We summarize and discuss our findings. A realistic model liquid in contact with a substrate that exerts a long-ranged van der Waals attraction undergoes a critical drying transition at zero attractive wall strength. From the general theory [19], we can infer that the same transition, at $\epsilon = 0$, should occur for models of water at such walls. Indeed the occurrence of critical drying would account for recent results [32–34, 38] displaying very large contact angles and enhanced fluctuations in simulations of water at strongly hydrophobic LR substrates.

Analysis of density fluctuations provides fresh insight into the nature of critical drying, revealing that (in simulations at least) there is only one divergent correlation length, $\xi_\parallel$, associated with the growth of vapor bubbles at the wall. Of course capillary wave theory predicts that $\xi_\perp$ diverges for a free interface in the absence of gravity, or at an infinite single wall in the limit of wetting/drying, but it seems one cannot observe a macroscopically large $\xi_\perp$ in fluid simulations, which therefore miss a key element of the theoretical picture [39]. It is tempting to speculate that a single diverging $\xi_\parallel$ could imply that critical drying in simulations is effectively controlled by the 2D Ising fixed point for which $\nu = 1$. This value is indeed much closer to our estimate of $\nu_\parallel$ than the predictions of RG theory for the LR case. Clearly further work is required to address these subtle but important issues.

Our methods for locating and characterizing critical drying should prove useful for elucidating critical wetting transitions in $d = 3$. Here fundamental questions remain regarding the relationship between simulation results and theoretical predictions [8, 9, 40–42]. In fig. 1 our results for $\cos(\theta)$ for a SR (square-well) wall indicate critical wetting. Preliminary investigations [43] of this system reveal closely analogous phenomenology to that seen at drying, namely a gas-peak in $p(\rho)$ which gradually disappears on increasing ϵ until, at the wetting point, $p(\rho)$ assumes a scale invariant form comprising a low density tail and a linear part extending to high density. The implication is that like critical drying, critical wetting in simulations will occur in the absence of a large $\xi_\perp$.

Our findings settle the long standing controversy regarding the order of the drying transition [10–16]. Furthermore they help explain the original misconception. This arose, we believe, because for fluids in a slit pore the liquid phase is metastable with respect to capillary evaporation (cf. the gas peak in the inset of fig. 2). As $\epsilon \to \epsilon_c(L)^+$, the liquid unbinds from the wall and the liquid-vapor interface wanders towards the slit center where it annihilates with its counterpart from the other wall to form a pure gas phase. In the absence of the insights provided by the present work, it is easy to mistake this discontinuous evaporation for the critical surface phase transition that precipitates it [10–12]. Note, however, that since the results of fig. 2 focus on the regime of moderate to large ρ they are unaffected by evaporation [44].

Finally, as regards the experimental relevance of our findings, the observation that the drying transition in liquids is critical irrespective of the range of the wall-fluid interactions, should prove important when interpreting observations of the properties of fluids near hydro- or solvo-phobic interfaces, in which there is growing technological [1–3] and fundamental [45, 46] interest. We do not expect the basic phenomenology of critical drying to be altered if one considers a substrate corrugated on the atomic scale rather than a planar one. It remains to be seen to what extent the phenomenology applies

for nanostructured surfaces with larger characteristic periods. Although real hydrophobic surfaces never quite attain contact angles $\theta = 180°$, the effects of criticality should extend over a wide range of $\theta < 180°$ [21, 27] and experiments such as those of ref. [47] might be able to confirm the existence of enhanced density fluctuations in the vicinity of a hydrophobic substrate.

R.E. acknowledges Leverhulme Trust grant EM-2016-031.

[1] J. T. Simpson, S. R. Hunter, and T. Aytug, Rep. Prog. Phys. **78**, 086501 (2015).

[2] X.-M. Li, D. Reinhoudt, and M. Crego-Calama, Chem. Soc. Rev. **36**, 1350 (2007).

[3] E. Ueda and P. A. Levkin, Adv. Mater. **25**, 1234 (2013).

[4] A. Checco, B. M. Ocko, A. Rahman, C. T. Black, M. Tasinkevych, A. Giacomello, and S. Dietrich, Phys. Rev. Lett. **112**, 216101 (2014).

[5] D. Bonn, J. Eggers, J. Indekeu, J. Meunier, and E. Rolley, Rev. Mod. Phys. **81**, 739 (2009).

[6] S. R. Friedman, M. Khalil, and P. Taborek, Phys. Rev. Lett. **111**, 226101 (2013).

[7] K. Binder, D. P. Landau, and S. Wansleben, Phys. Rev. B **40**, 6971 (1989).

[8] E. V. Albano and K. Binder, Phys. Rev. Lett. **109**, 036101 (2012).

[9] P. Bryk and K. Binder, Phys. Rev. E **88**, 030401 (2013).

[10] F. van Swol and J. R. Henderson, Phys. Rev. A **40**, 2567 (1989).

[11] J. R. Henderson and F. van Swol, J. Phys: Condens. Matter **2**, 4537 (1990).

[12] F. van Swol and J. R. Henderson, Phys. Rev. A **43**, 2932 (1991).

[13] M. J. P. Nijmeijer, C. Bruin, A. F. Bakker, and J. M. J. van Leeuwen, J. Phys: Condens. Matter **4**, 15 (1992).

[14] M. J. P. Nijmeijer, C. Bruin, A. F. Bakker, and J. M. J. van Leeuwen, Phys. Rev. B **44**, 834 (1991).

[15] J. R. Henderson, P. Tarazona, F. van Swol, and E. Velasco, J. Chem. Phys. **96**, 4633 (1992).

[16] C. Bruin, M. J. P. Nijmeijer, and R. M. Crevecoeur, J. Chem. Phys. **102**, 7622 (1995).

[17] F. Ancilotto, S. Curtarolo, F. Toigo, and M. W. Cole, Phys. Rev. Lett. **87**, 206103 (2001).

[18] A. Oleinikova, I. Brovchenko, and A. Geiger, J. Phys.: Condens. Matter **17**, 7845 (2005).

[19] R. Evans, M. Stewart, and N. Wilding, Supplementary material which also includes [48, 49] provides a) Details of Binding Potential calculations; b) Details of DFT calculation; c) Details of how the tails of $p(\rho)$ scale with the wall dimension L; d) A movie of the near critical interface.

[20] R. Evans, in *Fundamentals of Inhomogeneous Fluids*, edited by D. Henderson (Dekker, 1992) p. 85.

[21] R. Evans and M. C. Stewart, J. Phys.: Condens. Matt. **27**, 194111 (2015).

[22] B. A. Berg and T. Neuhaus, Phys. Rev. Lett. **68**, 9 (1992).

[23] N. B. Wilding, Phys. Rev. E **52**, 602 (1995).

[24] N. B. Wilding, J. Phys. Condens. Matter **28**, 414016 (2016).

[25] L. G. MacDowell, P. Virnau, M. Müller, and K. Binder, J. Chem. Phys. **120**, 5293 (2004).

[26] M. Müller and L. G. MacDowell, Macromolecules **33**, 3902 (2000).

[27] R. Evans and N. B. Wilding, Phys. Rev. Lett. **115**, 016103 (2015).

[28] S. Dietrich, *Phase Transitions and Critical Phenomena vol 12*, edited by C. Domb and J. L. Lebowitz (Academic, London, 1988).

[29] Y. Fan and P. A. Monson, J. Chem. Phys. **99**, 6897 (1993).

[30] P. Bryk, S. Sokołowski, and D. Henderson, J. Chem. Phys. **110**, 15 (1999).

[31] K. S. Rane, V. Kumar, and J. R. Errington, J. Chem. Phys. **135**, 234102 (2011).

[32] V. Kumar and J. R. Errington, Mol. Sim. **39**, 1143 (2013).

[33] V. Kumar and J. R. Errington, J. Phys. Chem. C **117**, 23017 (2013).

[34] A. P. Willard and D. Chandler, J. Chem. Phys. **141**, 18C519 (2014).

[35] P. Tarazona and R. Evans, Mol. Phys. **47**, 1033 (1982).

[36] R. Evans and A. O. Parry, J. Phys.: Condens. Matter **2**, SA15 (1990).

[37] M. P. Gelfand and M. E. Fisher, Physica A **166**, 1 (1990).

[38] R. Godawat, S. Jamadagni, V. Venkateshwara, and S. Garde, ArXiv:1409.2570.

[39] One should also note that, in simulation, the maximum thickness of the drying (vapour) layer that can be investigated is only a few atomic diameters.

[40] A. O. Parry, C. Rascón, N. R. Bernardino, and J. M. Romero-Enrique, Phys. Rev. Lett. **100**, 136105 (2008).

[41] A. O. Parry, C. Rascón, N. R. Bernardino, and J. M. Romero-Enrique, J. Phys.: Condens. Matter **20**, 494234 (2008).

[42] A. O. Parry and C. Rascón, J. Low Temp. Phys. **157**, 149 (2009).

[43] R. Evans, M. C. Stewart, and N. B. Wilding, unpublished results (2016).

[44] In a semi-infinite system, there is only a single vapor-liquid interface, which can wander arbitrarily far from the wall and the evaporation transition does not exist.

[45] M. Mezger, H. Reichert, B. M. Ocko, J. Daillant, and H. Dosch, Phys. Rev. Lett. **107**, 249801 (2011).

[46] A. Uysal, M. Chu, B. Stripe, A. Timalsina, S. Chattopadhyay, C. M. Schlepütz, T. J. Marks, and P. Dutta, Phys. Rev. B **88**, 035431 (2013).

[47] K. Nygård, S. Sarman, K. Hyltegren, S. Chodankar, E. Perret, J. Buitenhuis, J. F. van der Veen, and R. Kjellander, Phys. Rev. X **6**, 011014 (2016).

[48] M. P. Nightingale, W. F. Saam, and M. Schick, Phys. Rev. Lett. **51**, 1275 (1983).

[49] E. Brézin, B. I. Halperin, and S. Leibler, Phys. Rev. Lett. **50**, 1387 (1983).

SUPPLEMENTARY MATERIAL

Simulation Details

For our LJ fluid, particles interact via the potential,

$$\phi_{\rm att}(r) = \begin{cases} 4\epsilon_{LJ}\left[\left(\frac{\sigma}{r}\right)^{12} - \left(\frac{\sigma}{r}\right)^{6}\right], & r \le r_c\,, \\ 0, & r > r_c, \end{cases} \qquad (1)$$

with ϵ_{LJ} the well-depth of the potential and σ the LJ diameter. We choose $r_c = 2.5\sigma$, for which criticality occurs [23] at $k_BT_c = 1.1876(3)\epsilon_{LJ}$. We work at $k_BT = 0.91954\epsilon_{LJ} = 0.775T_c$ for which coexistence occurs at $\beta\mu_{co} = -3.865950(20)$, with coexistence densities $\rho_l\sigma^3 = 0.704(1)$ and $\rho_v\sigma^3 = 0.0286(2)$; and also at $k_BT_c = 1.0\epsilon_{LJ} = 0.842T_c$ for which $\beta\mu_{co} = -3.457131(25)$, $\rho_l\sigma^3 = 0.653(1)$, $\rho_l\sigma^3 = 0.0504(3)$.

We employ two types of wall-fluid potential in our GCMC simulations. The SR potential is a square-well given by

$$W_{\rm SR}(z) = \begin{cases} \infty, & z \le 0 \\ -\epsilon, & 0 < z < \sigma/2\,, \\ 0, & z > \sigma/2, \end{cases} \qquad (2)$$

where ϵ is the well-depth. The LR potential is given by

$$W_{\rm LR}(z) = \begin{cases} \infty, & z \le 0 \\ \epsilon_w\epsilon_{LJ}\left[\frac{2}{15}\left(\frac{\sigma}{\tilde{z}}\right)^{9} - \left(\frac{\sigma}{\tilde{z}}\right)^{3}\right], & z > 0\,, \end{cases} \qquad (3)$$

where $\tilde{z} = z + (2/5)^{1/6}\sigma$, use of which shifts the minimum of the 9-3 potential to the hard wall at $z = 0$. ϵ_w is a dimensionless measure of the strength of the wall-fluid attraction. At the minimum of (3) the value of the wall-fluid potential is $-1.0541\epsilon_w\epsilon_{LJ} = -\epsilon$.

Binding potential analysis for the LR case

We follow the standard treatment, e.g. [27], of wetting/drying transitions and consider $\omega^{ex}(l)$, the excess grand potential per unit surface area, as a function of the thickness l of the wetting/drying layer. For a truncated LJ model adsorbed at a single wall exerting the potential (3) we expect

$$\omega^{ex}(l) = \gamma_{wv} + \gamma_{lv} + \omega_B(l) + \delta\mu(\rho_l - \rho_v)l \qquad (4)$$

with the binding potential

$$\omega_B(l) = a\exp\left(-l/\xi_b\right) + bl^{-2} + \text{H.O.T.} \qquad (5)$$

ρ_l and ρ_v are the liquid and vapor densities at coexistence, $\delta\mu = \mu - \mu_{co} \ge 0$ is the deviation of the chemical potential from its value at coexistence and we have specialized now to the case of drying, i.e. l is the thickness of a layer of vapor that can intrude between the weakly attractive wall and the bulk liquid at $z = \infty$. In the limit of complete drying, at $\delta\mu = 0^+$, l diverges and the wl interface is a composite of the wv and lv interfaces. In this limit $\gamma_{wl} = \gamma_{wv} + \gamma_{lv}$, i.e. $\cos(\theta) = -1$. The binding potential in (4) has two leading contributions. The exponential term accounts for SR fluid-fluid interactions; ξ_b is the true correlation length of the bulk phase that wets, in our case the vapor, and a is a positive coefficient. The term bl^{-2} is associated with the z^{-3} decay of $W_{LR}(z)$ in (3); it arises from dispersion (van der Waals) forces between the substrate and the fluid. The higher order terms in (5) include higher inverse powers such as cl^{-3} as well as more rapidly decaying exponentials. We ignore these in the subsequent analysis. Making a straightforward sharp-kink approximation, or Hamaker type calculation, e.g. [27], yields

$$b = -(\rho_l - \rho_v)\epsilon_w\epsilon_{LJ}\sigma^3/2 \qquad (6)$$

Since $b < 0$ for all $T < T_c$, minimizing (4) w.r.t. l at $\delta\mu = 0^+$, leads to a finite value for the equilibrium thickness:

$$\frac{-l_{eq}}{\xi_b} = \ln\epsilon_w - 3\ln\left(\frac{l_{eq}}{\xi_b}\right) + \text{constants};\ \delta\mu = 0^+ \qquad (7)$$

A formula equivalent to (7) was derived by Nightingale *et al.* (see Eq. 6 of [48]) in a study of critical wetting in systems with LR forces. Those authors considered only the case where $\epsilon_w > 0$ and concluded there was no wetting, critical or first order. Here we focus on the situation where $\epsilon_w \to 0^+$, $b \to 0^-$ and l_{eq} diverges continuously. Note that for $\epsilon_w = 0$, $W_{LR}(z)$ reduces to the planar hard-wall potential and minimization of (4) then yields $-l_{eq}/\xi_b = \ln(\delta\mu) + \text{const}$, the mean-field (MF) result appropriate for complete drying from off-coexistence, for all $T < T_c$, e.g. [20, 28, 36].

Using (4,5) we can calculate several properties and examine these, within MF, in the approach to critical drying $\epsilon_w \to 0^+$. The local compressibility, evaluated for $z \approx l_{eq}$, is given by [21, 36]

$$\chi(l_{eq}) = \left(\frac{\partial\rho(z)}{\partial\mu}\right)_{z=l_{eq}} \sim -\rho'(l_{eq})\left(\frac{\partial l_{eq}}{\partial\mu}\right) \qquad (8)$$

where the prime denotes differentiation w.r.t. z. From (4) it follows that, at leading order,

$$\left(\frac{\partial l_{eq}}{\partial\mu}\right) = -\frac{\xi_b^2}{a}(\rho_l - \rho_v)\exp(l_{eq}/\xi_b);\ \delta\mu = 0^+ \qquad (9)$$

Capillary wave arguments predict that in the limit of critical drying $\rho'(l_{eq}) \sim \xi_\perp^{-1}$, where $\xi_\perp$ is the interfacial roughness. Within MF, $\xi_\perp^{-1}$ is non-zero, and using (7) we deduce

$$\ln \chi(l_{eq}) \sim \frac{l_{eq}}{\xi_b} + \text{const.}; \;\; \delta\mu = 0^+ \tag{10}$$

The predictions (7) and (10) were tested using the microscopic DFT, as described below.

We can also extract the correlation length $\xi_\parallel$ that describes density-density correlations parallel to the wall. General arguments, see Refs. [21, 36] and references therein, predict that $\xi_\parallel^2$ diverges in the same way as the surface excess compressibility defined as

$$\chi_{ex} \equiv \left(\frac{\partial \Gamma}{\partial \mu}\right) = \frac{\partial}{\partial \mu}\int_0^\infty dz(\rho(z) - \rho_b) = \int_0^\infty dz(\chi(z) - \chi_b) \tag{11}$$

where, $\rho_b = \rho(\infty)$ is the bulk density and Γ is the Gibbs adsorption. Since χ_{ex} is proportional to $-\partial l_{eq}/\partial\mu$ it follows from (9,7) that $\xi_\parallel$ diverges as

$$\xi_\parallel \sim \epsilon_w^{-1/2}(-\ln \epsilon_w)^{3/2}; \; \delta\mu = 0^+ \tag{12}$$

in the limit $\epsilon_w \to 0^+$. The same result is obtained from standard binding potential considerations [27] where one has $\xi_\parallel^{-2} \propto \partial^2\omega_B(l)/\partial l^2$ at $l = l_{eq}$.

The variation of $\cos(\theta)$ close to critical drying is determined by $\omega_B(l_{eq})$ at $\delta\mu = 0^+$, i.e. the singular part of the surface excess free energy γ^{sing}. Using Youngs equation one finds $1 + \cos(\theta) = -\omega_B(l_{eq})/\gamma^{lv}$ and for the present binding potential (5) we obtain

$$1 + \cos(\theta) \sim \epsilon_w(-\ln \epsilon_w)^{-2} \tag{13}$$

in the limit $\epsilon_w \to 0^+$. This result is striking. Were the logarithm not present in (13) the theory would predict $1 + \cos(\theta)$ vanishing linearly with ϵ_w, a signature of a 1st order drying transition. It is only the presence of the logarithm that ensures a continuous (critical) transition. The critical exponent α_s, defined by the vanishing of the singular part of the surface excess free energy $\gamma^{sing} \sim \epsilon_w^{2-\alpha_s}$, clearly takes the value $\alpha_s = 1$, with log corrections, in this particular case. The situation is similar to that for complete drying from off-coexistence where for a planar hard-wall, say, $\gamma^{sing} \sim \delta\mu \ln \delta\mu$, $\delta\mu \to 0^+$.

It is important to distinguish the MF scenario presented above from that corresponding to a SR wall-fluid potential such as (1). In the SR case it is well-known, e.g. [27,41], that the second inverse power-law term in (5) must be replaced by a H.O. term proportional to $\exp(-2l/\xi_b)$ while the coefficient of the leading $\exp(-l/\xi_b)$ term now depends on ϵ_w: $a(\epsilon_w) \sim (\epsilon_w - \epsilon_{wc}^{MF})$ where ϵ_{wc}^{MF} is the strength of the wall-fluid attraction at which critical drying occurs in MF. Defining $\delta\epsilon_w = \epsilon_w - \epsilon_{wc}^{MF}$, MF analysis for the SR case yields, for $\delta\mu = 0^+$,

$$\frac{-l_{eq}}{\xi_b} \sim \ln(\delta\epsilon_w); \;\; \chi(l_{eq}) \sim (\delta\epsilon_w)^{-2}; \;\; \xi_\parallel \sim (\delta\epsilon_w)^{-1} \tag{14}$$

and

$$1 + \cos(\theta) \sim (\delta\epsilon_w)^2 \;\; \text{or} \;\; \alpha_s = 0; \tag{15}$$

These results are clearly very different from those we obtained above for the LR case.

A Renormalization Group (RG) treatment of fluctuations

The analysis described above was strictly MF; this omits some of the effects of capillary wave (CW) fluctuations. For example, for infinite surface area, MF predicts a sharp interface with $\xi_\perp$ finite in all dimensions d whereas, in reality, we expect $\xi_\perp$ to diverge for $d \leq 3$. An important early attempt to incorporate CW fluctuations was that of Brezin et al. [49] who introduced a RG treatment for the case of SR forces where the upper critical dimension is $d = 3$ for both critical wetting and complete wetting from off-coexistence. We follow their methodology for our binding potential (5).

First we invoke the hyperscaling relation $(2 - \alpha_s) = (d - 1)\nu_\parallel$, where $\nu_\parallel$ is the critical exponent for $\xi_\parallel$, insert the MF exponents given above and deduce that the upper critical dimension is, once again, $d = 3$. Next we introduce the standard, dimensionless parameter $\omega = (4\pi\beta\gamma_{lv}\xi_b^2)^{-1}$, with $\beta = (k_BT)^{-1}$, that measures the strength of CW fluctuations. The RG treatment then implies we should consider an effective binding potential (renormalized) at the scale $\xi_\parallel$:

$$\omega_{\xi_\parallel}(l) = a\xi_\parallel^\omega \exp(-l/\xi_b) + bl^{-2} + \delta\mu(\rho_l - \rho_v)l \tag{16}$$

The exponential term is renormalized but the remaining power-law terms are not; in particular the coefficient b is assumed to be unchanged. Minimization of (16) yields

$$-\frac{l_{eq}}{\xi_b} = (1 + \frac{\omega}{2})(\ln \epsilon_w - 3\ln(l_{eq}/\xi_b)); \;\; \delta\mu = 0^+ \tag{17}$$

as $\epsilon_w \to 0^+$. The equilibrium thickness still diverges with the MF form (7) but the amplitude is increased by a factor $(1 + \omega/2)$. MF is recovered when the interface becomes very stiff so that $\omega \to 0$. The parallel correlation length can be obtained from either $\xi_\parallel^{-2} \propto \left(\frac{\partial^2\omega_B(l)}{\partial l^2}\right)$ at $l = l_{eq}$ or from $\xi_\parallel^2 \propto \left(\frac{\partial l_{eq}}{\partial\mu}\right)$. In both cases we find

$$\xi_\parallel \sim \epsilon_w^{-1/2}[(1 + \frac{w}{2})(-\ln \epsilon_w)]^{3/2}; \;\; \delta\mu = 0^+ \tag{18}$$

The singular part of the surface excess free energy can be calculated from (16) and we obtain

$$1+\cos(\theta) \sim \epsilon_w(-(1+\frac{\omega}{2})\ln\epsilon_w)^{-2};\;\; \delta\mu = 0^+ \qquad (19)$$

Once again only the amplitudes are changed from the MF results (12) and (13). Note that (17) is reminiscent of the result for complete drying from off-coexistence for SR forces, e.g. at a planar hard-wall. There the second term in (16) is absent but the third remains leading to

$$-\frac{l_{eq}}{\xi_b} = (1+\frac{\omega}{2})\ln\delta\mu, \text{as } \delta\mu \to 0^+ \qquad (20)$$

Unlike the case of SR forces considered by Brezin et al. [49] and in many subsequent studies, e.g. [7, 8, 40–42] where several of the critical exponents are predicted to depend explicitly on the parameter ω, for the binding potential (5) our RG analysis predicts the critical exponents to be unchanged from their MF values and therefore independent of ω even though the upper critical dimension is also $d = 3$. We note that the conclusions of the MF and RG analyzes are changed little if we consider LR wall-fluid potentials other than the standard 9-3 case (3). Suppose the leading power-law decay is proportional to $-(\sigma/z)^p$, with $p > 2$. Then the coefficient of the logarithm in (7) is replaced by $(p+1)$, (10) is unchanged, and the power of the logarithm in (12) and (13) is replaced by $(p+1)/2$ and $-p$, respectively. The RG results are changed accordingly.

Details of DFT calculations

The classical DFT that we employ is that used in a previous study of solvophobic substrates but one that did not address critical drying [21]. The excess Helmholtz free energy functional is approximated by the sum of a hard-sphere functional, treated by means of Rosenfeld's fundamental measure theory, and a standard MF treatment of attractive fluid-fluid interactions. Eq.(14) of Ref. [21] displays the grand potential functional. In the present study the attractive part of the truncated LJ potential is given by

$$\phi_{\rm att}(r) = \begin{cases} -\epsilon_{LJ}, & r < r_{\rm min} \\ 4\epsilon_{LJ}\left[\left(\frac{\sigma}{r}\right)^{12} - \left(\frac{\sigma}{r}\right)^{6}\right], & r_{\rm min} < r < r_c\,, \\ 0, & r > r_c, \end{cases} \qquad (21)$$

where $r_{\rm min} = 2^{1/6}\sigma$. The potential is truncated at $r_c = 2.5\sigma$, as in simulation. The critical temperature is given by $k_BT_c = 1.3194\epsilon_{LJ}$ and calculations are performed at $T = 0.775T_c$. The wall-fluid potential is the standard 9-3 model:

$$W_{93}(z) = \epsilon_w\epsilon_{LJ}\left[\frac{2}{15}\left(\frac{\sigma}{z}\right)^9 - \left(\frac{\sigma}{z}\right)^3\right], \qquad (22)$$

where, once again, ϵ_w is a dimensionless measure of the ratio of the wall-fluid attraction compared to that of fluid-fluid. Note that (22) differs slightly from (3). However, the crucial z^{-3} tail contribution has the same coefficient. The hard-sphere diameter, entering the functional, is $d = \sigma$.

In the calculations we determine equilibrium density profiles $\rho(z)$ and the surface tensions $\gamma_{lv}, \gamma_{wl}, \gamma_{wv}$, by minimizing the grand potential functional [21]. The local compressibility $\chi(z)$ is determined numerically as described in [21]. We have performed calculations for a single wall and for a pair of confining walls, equivalent to the GCMC simulations. In this Letter we show results for the single wall only.

Key results are shown in Fig. S1 below. Here we plot $\rho(z)$ and $\chi(z)$ for very small values of ϵ_w. As ϵ_w is reduced towards zero the thickness of the drying film l_{eq} increases (panel 1). We have confirmed in detail, within DFT, that the Gibbs adsorption or l_{eq} grows according to (7). The position of the peak in $\chi(z)$ shifts with the position of the gas-liquid interface and its height increases very rapidly as $\epsilon_w \to 0^+$ (panel 2). Panel 3 shows clearly that $\ln\chi(l_{eq})$ increases linearly with l_{eq}. The prediction (10), including the correct prefactor, the inverse bulk correlation length, is confirmed by our DFT calculations. We determine the contact angle via Young's equation and DFT results for $\cos(\theta)$ are shown in the right panel of Fig. 1 (main text). For the LR case (22) we find critical drying at $\epsilon_w = 0$ and 1st order wetting at a value of ϵ_w that is smaller than in simulation. For the SR case (square-well), where again $d = \sigma$, both drying and wetting are critical transitions, as in simulation. However, the separation in ϵ_w between wetting and drying in DFT is smaller than in simulation. In summary the microscopic DFT results for a single wall are in complete agreement with those from the simple binding potential treatment, based on (5), and described above.

L-dependence of the high density tail of $p(\rho)$

The high density tail in $p(\rho)$ corresponds to the free energy cost of pushing the liquid-slab up against the hard wall. A clear feature of Fig. 2 is that the density at which the tail occurs shifts strongly to lower values as the wall area L^2 increases. One complication in comparing the distributions for various L to explain this shift is that sampling of $p(\rho)$ is truncated at low densities due to the need to avoid the region of capillary evaporation. Consequently it is not possible to normalize the distribution. To deal with this (and to make the tails more visible) let us instead consider the logarithm of $p(\rho)$ which is the negative of the (grand) free energy function $F(\rho) = -k_BT\ln p(\rho)$. Doing so changes the unknown normalization factor into an additive constant, which can be removed by differentiation. The derivative $\partial\ln p(\rho)/\partial\rho$, is closely related to

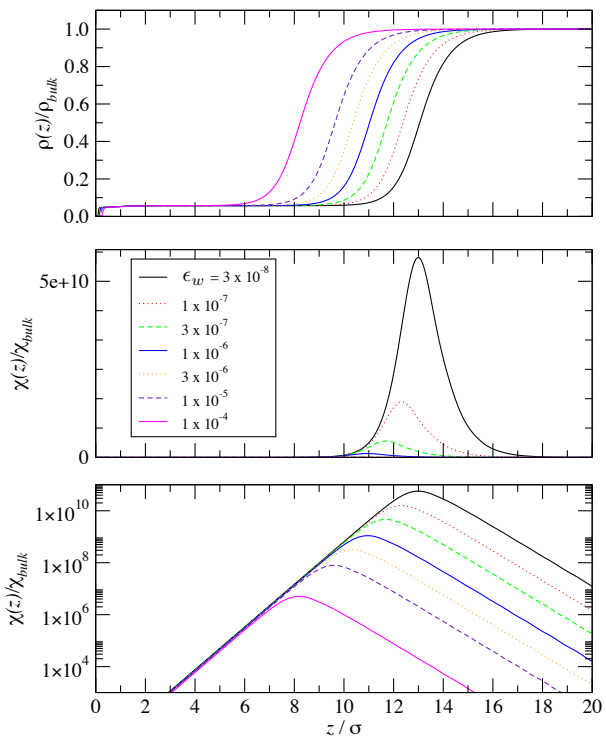

FIG. S1. DFT results for the normalised density profiles $\rho(z)/\rho_b$ (top panel) and the local compressibilities $\chi(z)/\chi_b$ (linear scale - middle panel; log-scale - bottom panel) for the fluid at single walls. The strength of the wall-fluid interaction potentials are given in the caption. The temperature is $T = 0.775T_c$ and the reservoir is at bulk liquid-gas coexistence, on the liquid side $\delta\mu = 0^+$.

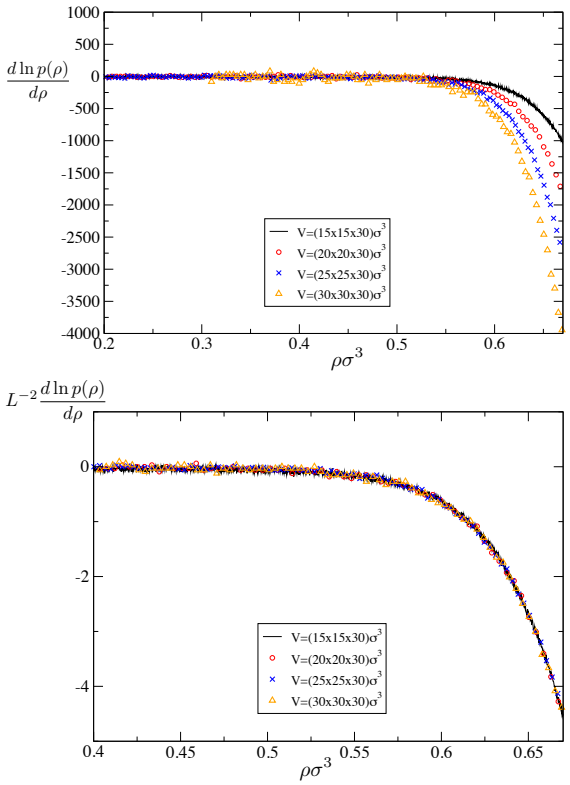

FIG. S2. **(a)** $\partial \ln p(\rho)/\partial\rho$ for $L = 15\sigma, 20\sigma, 25\sigma, 30\sigma$ at $\epsilon = 0$ and $T = 0.775T_c$. **(b)** The same data scaled by L^{-2}

$\mu(N) = -k_BT(\partial \ln p(N)/\partial N)$, the chemical potential function. A plot of this derivative is given in Fig. S2. We find that the curves all scale onto one another with a simple L^{-2} scaling of the ordinate, no scaling is needed for the density. In view of this, we can write

$$\frac{\partial \ln p(\rho)}{\partial \rho} = L^2 g(\rho) \tag{23}$$

where $g(\rho)$ is some function of ρ. It follows that the free energy itself scales like

$$-\ln p(\rho) = -L^2 \int_0^\rho g(\rho')d\rho' \tag{24}$$

i.e. it has a rather trivial L^2 scaling.

An appealing rationalization of this finding is in mechanical terms. The configuration takes the form of a liquid slab. For the density to grow, the slab has to thicken, i.e the slab interface has to approach the hard walls. Thus the density is linearly related to the average separation of the slab surface from the walls ie. $\rho \propto z$. From this viewpoint, $\partial \ln p(\rho)/\partial\rho$ is a force profile and $g(\rho)$ is a pressure profile. The L^2 scaling then suggest that the hard wall exerts a repulsive pressure on the liquid-vapor interface which is independent of L, so the force (and hence the work) required to push the interface to the walls increases like L^2. The L^2 scaling of the free energy leads to the apparent shift in the tail position in $p(\rho)$.

Movie of the emergent liquid-vapor interface near critical drying

This movie (from which the snapshot of fig. 4 was taken) allows a clearer view of the configurational structure that occurs near critical drying. The movie focuses on the region near the wall at $z = 0$ for a system of size $L = 40\sigma$. The temperature is $T = 0.775T_c$ and the attractive wall strength is $\epsilon = 0.2$ which is slightly larger than that for which the liquid peak in $p(\rho)$ vanishes for this L. Observing the purple shaded particles lying close to the wall we note that there is a large but finite $\xi_{||}$ manifest in the large fractal bubbles of 'vapor' which almost span the system in the lateral dimension. However, the perpendicular extent of these bubbles is microscopic, extending only a few particle diameters away from the wall. `<http://people.bath.ac.uk/pysnbw/sm_movie.mp4>`